9. W. J. Nellis and M. B. Brodsky, in *The Actinides: Electronic Structure and Related Properties*, A. J. Freeman and J. B. Darby, Eds. (Academic Press, New York, 1974), vol. 2, p. 265.
10. H. H. Hill, J. D. G. Lindsay, R. W. White, L. B. Asprey, V. O. Struebing, B. T. Matthias, *Physica* **55**, 615 (1971); H. H. Hill and F. H. Ellinger, *J. Less-Common Met.* **23**, 92 (1971).
11. J. W. Ward and H. H. Hill, in *Heavy Element Properties*, W. Müller and H. Blank, Eds. (North-Holland, Amsterdam, 1976), p. 65.
12. G. Gladstone, M. A. Jensen, J. R. Schrieffer, *Superconductivity*, R. D. Parks, Ed. (Dekker, New York, 1969), p. 665.
13. We thank B. T. Matthias, J. W. Ward, B. Johannson, M. B. Brodsky, and B. W. Veal for helpful discussions. Work was performed under the auspices of the Department of Energy.

13 February 1978

Fluorinated Molecule as a Tracer: Difluoroserotonin in Human Platelets Mapped by Electron Energy-Loss Spectroscopy

Abstract. *The intracellular distribution of fluorine has been delineated in human platelets incubated with 4,6-difluoroserotonin, utilizing a scanning-transmission electron microscope equipped with an energy-loss spectrometer. Discrete intracellular structures corresponding in location to dense bodies contained high concentrations of fluorine. Electron energy-loss spectroscopy, which apparently can detect less than 10^{-20} gram of fluorine in an area of 10 square nanometers, can thus localize fluorinated tracer molecules with biological activity.*

Fluorinated analogs of biologically significant organic molecules have proved to be extremely valuable biochemical and pharmacological agents. Substitution of fluorine for hydrogen introduces no serious steric alteration into the molecule, and the fluorinated analog frequently is recognized as its natural relative by enzymes, receptors, or transport systems (*1*). Continued synthetic activity in the area of organofluorine chemistry, which has provided a wide variety of fluorinated organic molecules, reflects the importance of these analogs (*2*).

In theory, fluorine associated with an organic molecule should provide an excellent tracer for determining at an ultrastructural level the distribution within the cell of a number of soluble compounds of importance in cellular function. Virtually no fluorine is present in cells under normal circumstances, and the substituent often allows an intracellular disposition mimicking that of the parent compound. This potential application of fluorinated compounds has been seriously hampered, however, by the lack of a suitable method for localizing fluorine inside cells. Conventional x-ray microanalysis systems, for example, are relatively insensitive to fluorine (*3*). We report that electron energy-loss spectroscopy, which we have utilized to localize a fluorinated analog of serotonin (5HT) sequestered intracellularly in human platelets, appears to provide a sensitive and specific method for the detection of fluorine in biological systems (*4*).

4,6-Difluoroserotonin (DF5HT) was synthesized by a method described elsewhere (*5*). The tritiated compound was prepared by acid-catalyzed decarboxylation of 4,6-difluoro-5-methoxytryptamine-2-carboxylic acid in tritiated water (5 Ci/ml), followed by demethylation. The intracellular disposition of tritiated DF5HT was compared with that of tritiated 5HT in human platelets by use of brief thrombin treatment and formaldehyde fixative to evaluate the amount of labeled material in the thrombin-releasable (vesicular) and non-thrombin-releasable (cytoplasmic) compartments of washed platelets (*6–8*) (Table 1). Although there are some differences in the behavior of the two compounds (*9*), comparable amounts of [^{3}H]DF5HT and [^{3}H]5HT enter platelet vesicles and cytoplasm at all time points and concentrations. Thus the intracellular sequestration of [^{3}H]DF5HT can provide a useful index for the compartmentation of [^{3}H]5HT.

Before electron microscopy, platelets were incubated for 60 minutes with an initial concentration of $10^{-5}M$[^{3}H]-DF5HT. When measured with thrombin and fixative as described above, cells contained on the average 1.9×10^{-17} mole per platelet of [^{3}H]DF5HT in a vesicular compartment and 0.2×10^{-17} mole per platelet in a cytoplasmic compartment. After incubation, platelets were air-dried by rapid blotting on copper grids coated with collodion and carbon, a procedure employed previously to analyze the content and distribution of platelet dense bodies (*6, 7, 10, 11*). Grids were examined at 100 kV in a JEOL JEM-100B electron microscope equipped with a scanning attachment, an electron spectrometer, and a Kevex multichannel analyzer (*12*). As imaged by utilizing all the transmitted electrons in the scanning-transmission electron microscopy (STEM) mode (spot size, 10 nm^2), most platelets contained dense bodies, which appeared dark because of their high calcium content and total scattering power (*6, 7, 10, 11*). Energy-loss spectra obtained from dense bodies probed with a 10-nm^2 stationary spot showed large fluorine ionization edges at

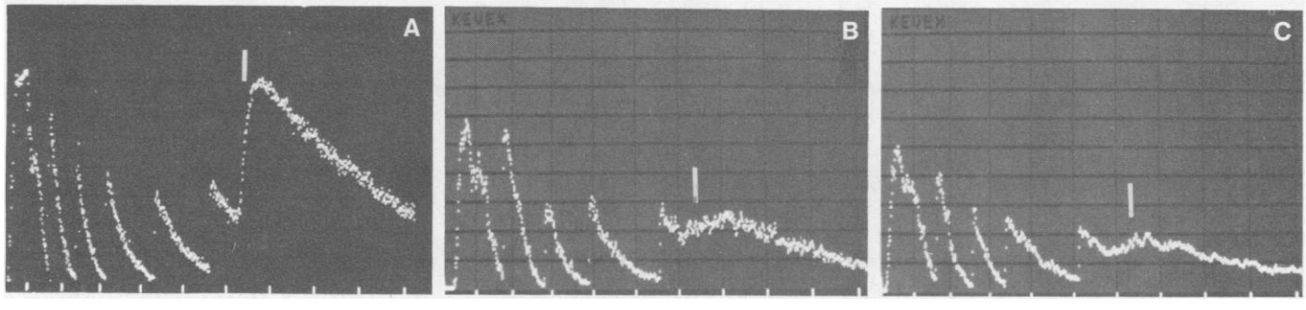

Fig. 1. Energy-loss spectra recorded from various portions of a platelet incubated with DF5HT. The region corresponding to an average loss of 680 eV (characteristic of fluorine *K*-shell ionization) is marked with a bar. The analysis system compensates for differences between the numbers of zero-loss and 680 eV-loss electrons by increasing the gain of the photomultiplier tube as the electron beam is scanned from zero loss to 680 eV loss. Thus, the breaks in the spectra at approximately 100-eV intervals represent points at which the gain of the photomultiplier tube was increased. Regardless of gain at 680 eV, the integral area of the peak rising above the descending curve of the background contribution is approximately proportional to the number of fluorine molecules interacting with the incident electron beam. (A) Spectrum recorded from a dense body. A prominent absorption edge for fluorine is present. (B) Spectrum from the cytoplasmic apron (organelle-free region) of a platelet. A small fluorine edge is present. (C) Spectrum from the supporting film immediately adjacent to the platelet. A very small fluorine edge is present.

0036-8075/78/0505-0537$00.50/0

680 eV (Fig. 1A) (*13*). Spectra obtained from areas of platelet cytoplasm well removed from dense bodies contained significant but much smaller fluorine edges (Fig. 1B). Spectra obtained from the supporting film near platelets contained even smaller fluorine edges (Fig. 1C); and spectra from grid squares with no platelets contained no discernible fluorine edges.

Total scattering images of the same cells obtained in the STEM mode were compared with those obtained by utilizing only electrons that had lost 680 eV, a condition under which the image is formed by electrons with an average energy loss corresponding to the *K*-shell ionization of fluorine (Fig. 2). As seen in the total scattering image, cells contained both dense bodies and a number of electron-lucent areas [which appear to represent intracellular vacuoles (*14*)]. As imaged in the 680 eV-loss mode, dense bodies became highly lucent and intracellular vacuoles became dark. The cell cytoplasm and the layer of material surrounding the cell perimeter became more lucent than vacuoles, adjacent grid bars, and areas of grid film well removed from platelets.

Variations in mass thickness over different regions of the cell can give rise to contrast differences between various regions. Theoretically, this effect should not contribute significantly to the contrast differences seen in the 680 eV-loss mode, since the electron mean free path for mass thickness scattering is of the order of micrometers, compared to a maximum specimen thickness of 100 to 200 nm (*14*). Thus in practice the relative lucency of a particular area in the 680 eV-loss image should be approximately proportional to its fluorine content. In keeping with this hypothesis, when the spectrometer was adjusted to image the same cells, using only electrons that had lost 620 eV (a value just below the fluorine edge), the entire cell was almost indistinguishable from the grid film.

In a particular cell seen in the 680 eV-loss mode, all the identifiable dense bodies and the entire dense-body area (including even the tail in dense bodies associated with these structures) were lighter than the surrounding cytoplasm. Cells incubated with 5HT and containing dense bodies were not distinguishable from the background in the 680 eV-loss mode. Cells incubated with DF5HT but containing no dense bodies revealed no highly lucent areas when imaged in the 680 eV-loss mode (*15*).

Table 1. Comparison of the sequestration of [^{3}H]5HT and [^{3}H]DF5HT in vesicles of intact human platelets. Each value is the mean of eight separate determinations.

Initial concentration and incubation time	Labeled material present (mole per platelet $\times 10^{18}$)			
	[^{3}H]5HT		[^{3}H]DF5HT	
	Total	Vesicular	Total	Vesicular
$10^{-6}M$				
30 seconds	0.27	0.10	0.31	0.14
30 minutes	2.66	2.66	2.26	1.84
$10^{-5}M$				
30 seconds	0.41	0.12	0.62	0.20
60 minutes	17.6	16.0	16.7	13.7

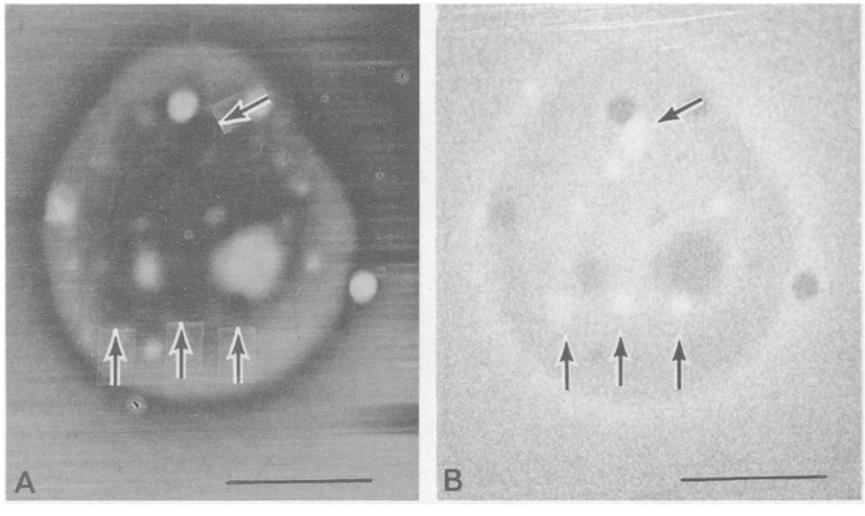

Fig. 2. Scanning-transmission electron microscopic images of a platelet incubated with DF5HT and air-dried. Scale bars, 1.0 μm. (A) Image formed with all the transmitted electrons. Dark circular or ovoid structures (arrows) are dense bodies and clear intracellular areas are believed to represent vacuoles. (B) Image formed with only electrons having an average energy loss of 680 eV. Dense bodies (arrows) are highly electron-lucent, and vacuoles are dark. The cell cytoplasm is intermediate in lucency between these two structures. The cell is also surrounded by a rim of lucent material.

Although definitive proof is lacking, several lines of evidence suggest that the 5HT-containing vesicular compartment is represented exclusively by dense bodies (*6, 7, 11, 16*). Our results define more precisely the correspondence between dense bodies and the vesicular storage site, since cells containing high concentrations of [^{3}H]DF5HT in their vesicular compartment also contain high concentrations of fluorine in their dense bodies. The same cells, which contain much less [^{3}H]DF5HT in their cytoplasmic compartment, contain much lower (but still detectable) concentrations of fluorine in organelle-free cytoplasm, as measured either by probing or by mapping in the 680 eV-loss mode. The fluorine-containing material that appears to surround and lie immediately adjacent to cells may be DF5HT trapped by platelet glycocalyx or by protein in the extracellular medium during the air-drying process. At present, we have no way to determine whether some of this material may also come from rapid movement of cytoplasmic material to the outside as the cell is dehydrated.

This work illustrates some particular advantages of the use of electron energy-loss spectroscopy to study the intracellular distribution of fluorinated organic molecules. The fluorine 680-eV edge is well removed from the low-energy loss region of the spectrum, and the inelastic electron mean free path at 680 eV is several micrometers, a value much greater than the thickness of biological specimens which can be imaged at 100 kV. In addition, the contribution of plasmon electrons to the electron spectrum at 680 eV is probably less than a few percent, with the result that the peak-to-background ratio in the spot-analysis mode is of the order of two or three to one (integrating over an energy window of 200 eV). Accordingly one can be confident that an absorption edge at 680 eV indicates the presence of fluorine. In the platelets examined here, the organelle-free region is about 20 to 40 nm thick (*14*). A 10-nm^2 spot size focused in this region gives an identifiable fluorine edge. Assuming that the nonreleasable cytoplasmic pool of 0.4×10^{-17} mole of fluorine per platelet is evenly distributed in the living cell throughout the platelet volume of approximately 7×10^7 nm^3, we can calculate that the entire illuminated volume of 3×10^5 nm^3 in the dried cell might contain as much as 2×10^{-21} g of fluorine.

In the 680 eV-loss mapping mode, the assignment of an absolute sensitivity is difficult with the limited data we have obtained. Nevertheless, the technique ap-

pears to be capable of discriminating between DF5HT-containing cytoplasmic areas and intracellular vacuoles. Qualitatively, the mapping mode is extremely useful in selecting fluorine-rich areas for subsequent study by specific probing. Although the spatial resolution of 10 to 30 nm and the signal-to-noise levels obtained here by mapping cannot be compared directly to those obtainable by either x-ray microanalysis or electron microscope radioautography, they appear to be superior to those obtained from biological specimens with the latter two techniques. A combination of mapping and probing with energy-loss spectroscopy should thus permit the determination in biological material of the intracellular disposition and translocations of a wide range of fluorinated organic molecules.

JONATHAN L. COSTA
Clinical Neuropharmacology Branch, National Institute of Mental Health, Bethesda, Maryland 20014
DAVID C. JOY
DENNIS M. MAHER
Bell Laboratories, Murray Hill, New Jersey 07974
KENNETH L. KIRK
Laboratory of Chemistry, National Institute of Arthritis, Metabolism, and Digestive Diseases, Bethesda, Maryland 20014
S. W. HUI
Department of Biophysics, Roswell Park Memorial Institute, Buffalo, New York 14263

References and Notes

1. P. Goldman, *Science* **164**, 1123 (1969); D. F. Loncrini and R. Filler, *Adv. Fluorine Chem.* **6**, 43 (1970); R. Filler, Ed., *Biochemistry Involving Carbon-Fluorine Bonds* (American Chemical Society, Washington, D.C., 1976).
2. G. A. Boswell, Jr., W. C. Ripka, R. M. Scribner, *Org. React.* **21**, 1 (1974); C. M. Sharts and W. A. Sheppard, *ibid.*, p. 125; M. J. Shaw, J. A. Weil, H. H. Hyman, R. Filler, *J. Am. Chem. Soc.* **92**, 5096 (1970); K. L. Kirk and L. A. Cohen, *ibid.* **95**, 4619 (1973).
3. R. Woldseth, *X-Ray Energy Spectrometry* (Kevex Corp., Burlingame, Calif., 1973).
4. M. Isaacson and D. Johnson, *Ultramicroscopy* **1**, 33 (1975); C. Colliex, V. E. Cosslett, R. D. Leapman, P. Trebbia, *ibid.* **1**, 301 (1976); M. S. Isaacson and A. V. Crewe, *Annu. Rev. Biophys. Bioeng.* **4**, 165 (1975).
5. K. L. Kirk, *J. Heterocyclic Chem.* **13**, 1253 (1976).
6. J. L. Costa and D. L. Murphy, *Nature (London)* **255**, 407 (1975).
7. ———, *Life Sci.* **18**, 1413 (1976).
8. ———, M. Kafka, *Biochem. Pharmacol.* **26**, 517 (1977).
9. J. L. Costa, K. L. Kirk, H. Stark, D. L. Murphy, in preparation.
10. J. L. Costa, T. S. Reese, D. L. Murphy, *Science* **183**, 537 (1974); J. L. Costa, Y. Tanaka, K. D. Pettigrew, R. J. Cushing, *J. Histochem. Cytochem.* **25**, 1079 (1977).
11. J. L. Costa, T. C. Detwiler, R. D. Feinman, D. L. Murphy, C. S. Patlak, K. D. Pettigrew, *J. Physiol. (London)* **264**, 297 (1977).
12. To maximize the signal-to-noise ratio, the electron spectrometer was operated with an acceptance angle of 5 mrad and a slit width chosen to give a resolution of 20 eV. These values were chosen to permit good separation of the *K* and *L* edges of all elements [D. C. Joy and D. M. Maher, *Proc. Electron Microsc. Soc. Am. 35th* (1977), p. 244].
13. During the recording of a single spectrum, cells were exposed to the 10-nm² spot for approximately 10 seconds (specimen-level current density, 10 A/cm²). Recording a second and third spectrum with the beam positioned identically gave fluorine absorption edges with the same integral area as that seen in the first spectrum. Thus, under the conditions employed here, loss of fluorine due to radiation damage appears not to present a problem.
14. S. W. Hui and J. L. Costa, in preparation.
15. We also examined platelets incubated for 60 minutes with an initial concentration of $10^{-5}M$ of the sulfur analog of serotonin [the benzo[*b*]thiophene derivative of 5HT; see E. Campaigne, D. R. Knapp, E. S. Neiss, T. R. Bosin, *Adv. Drug Res.* **5**, 1 (1970); T. R. Bosin and E. Campaigne, *ibid.*, in press]. Spectra recorded from dense bodies in these cells contained large sulfur ionization edges at 240 eV, but no fluorine edges. In addition, dense bodies were lucent when cells were mapped in the 240 eV-loss mode, but not in the 680 eV-loss mode.
16. J. G. White, *Ser. Haematol.* **3**, 17 (1970); J. L. Costa and S. W. Hui, *Biophys. J.* **19**, 307 (1977).
17. S.W.H. is the recipient of a career development award (CA 00084) from the National Cancer Institute. We thank M. A. Smith for technical assistance.

13 October 1977; revised 9 January 1978

Ah Locus: Genetic Differences in Susceptibility to Cataracts Induced by Acetaminophen

Abstract. *The Ah^b/Ah^b homozygous and the Ah^b/Ah^d heterozygous inbred mouse strains from the (C57BL/6)(DBA/2)F_1 × DBA/2 backcross are genetically responsive to 3-methylcholanthrene. They both also develop, within 6 hours after a large intraperitoneal dose of acetaminophen, an irreversible opacity in the anterior portion of the lens. Such cataract formation does not occur in similarly treated nonresponsive inbred strains or nonresponsive Ah^d/Ah^d individuals from the same backcross. Differences in acetaminophen metabolism and toxicity are associated with the Ah locus in the mouse, and differences in heritability at the Ah locus exist in the human. Our ophthalmologic findings may be important clinically to certain patients receiving either a single large overdose of this drug or high doses over a long period.*

Lenticular opacification or cataract results from senility, congenital defects, viral infections, metabolic disorders, and various types of physical and chemical insult to the lens (*1*). Cataracts can also be induced in lenses in organ culture (*2*). Because of the diversity in cataractogenic agents, no single mechanism can account for the different forms of cataract. Osmotic imbalance produced by polyol accumulation within the lens was suggested to be responsible for sugar-induced cataract (*3*), and light-scattering by aggregated protein was suggested as a cause of senile cataracts (*4*). Cataracts induced by chemicals and drugs, especially naphthalene, have been extensively investigated because of their similarity to senile cataracts (*5*).

The Ah locus in the mouse controls the ability of polycyclic and halogenated aromatic compounds to induce the monooxygenase activities associated with cytochrome P_1-450 (*6*, *7*). The Ah

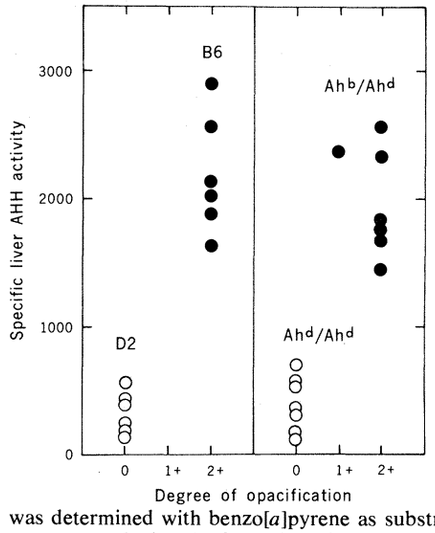

Fig. 1. Correlation between hepatic AHH inducibility and cataractogenesis in the nonresponsive D2 inbred strain, the responsive B6 inbred strain, and the nonresponsive Ah^d/Ah^d and responsive Ah^b/Ah^d progeny from the B6D2F_1 × D2 backcross. All inbred mice were obtained from The Jackson Laboratory (Bar Harbor), and all breeding was done within our own mouse colony. Sexually immature (5- to 6-week-old) mice of either sex were used. The mice were treated intraperitoneally with MC (200 mg per kilogram of body weight) in corn oil (25 ml/kg) 48 hours prior to acetaminophen (1000 mg/kg) in warm water (25 ml/kg). The acetaminophen was completely dissolved at the time of injection. No mice died before 6 hours at this dose. Eyes were evaluated with an ophthalmology slit lamp 5 hours later: 0, no signs of opacification; 1+, about 50 percent opacification; 2+, complete opacification. Mice were then immediately killed, and liver microsomal AHH activity was determined with benzo[*a*]pyrene as substrate (*18*). One unit is defined as that amount of enzyme catalyzing the formation of the hydroxylated product per minute at 37°C causing fluorescence equivalent to that of 1 pmole of 3-hydroxybenzo[*a*]pyrene (*18*). Specific AHH activity denotes the number of units per milligram of microsomal protein. Seven nonresponsive Ah^d/Ah^d and seven responsive Ah^b/Ah^d weanlings from the B6D2F_1 × D2 backcross were genotyped with respect to the Ah locus by zoxazolamine paralysis time (*19*); these mice were then given MC and acetaminophen 2 weeks later.

0036-8075/78/0505-0539$00.50/0